Advanced Synthesis & Catalysis

Accepted Article

Title: Decarboxylative Synthesis of Functionalized Oxindoles via A Iron-Initiated Radical Chain Process and Application to Construction of Diverse Fused-Indoline Heterocycles

Authors: Zhihao Cui and Da-Ming Du

To be cited as: *Adv. Synth. Catal.* 10.1002/adsc.201700976

Link to VoR: http://dx.doi.org/10.1002/adsc.201700976

COMMUNICATION

DOI: 10.1002/adsc.201((will be filled in by the editorial staff))

Decarboxylative Synthesis of Functionalized Oxindoles via An Iron-Initiated Radical Chain Process and Application in Constructing Diverse Fused-Indoline Heterocycles

Zhihao Cui and Da-Ming Du*

School of Chemistry and Chemical Engineering, Beijing Institute of Technology, Beijing 100081, People's Republic of China
e-mail: dudm@bit.edu.cn

Received: ((will be filled in by the editorial staff))

Supporting information for this article is available on the WWW under http://dx.doi.org/10.1002/adsc.201######.((Please delete if not appropriate))

Abstract. Rapid construction of diverse fused-indoline−heterocycle (FIH) frameworks including high-value pyrroloindolines, furoindolines and thienoindolines in a two-step sequence has been described. The key to success hinges on the adoption of peresters as α-heteroatom alkyl radical precusors, which can smoothly react with *N*-arylacrylamides via a radical chain process initiated by inexpensive $FeCl_2·4H_2O$ to afford the functionalized oxindoles, the key intermediates to FIH skeletons. The approach features operationally-simplicity, broad substrates scope and mild conditions.

Keywords: $FeCl_2·4H_2O$; Peresters; Oxindoles; Fused-indoline−heterocycle skeletons; Electron catalysis

In the total known indole alkaloids so far, those bearing the fused-indoline−heterocycle (FIH) skeletons, such as pyrroloindoline and furoindoline (Figure 1), hold a large proportion. These tricyclic indole alkaloids usually display various bioactivities,[1] ranging from acetyl cholinesterase inhibitors[2], antibacterial[3a] and anticancer activity[3b] to potential drug candidates for Alzheimer's disease.[4]

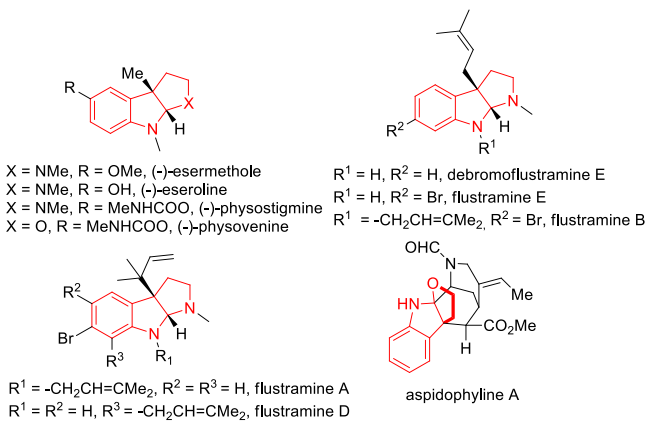

Figure 1. Indole Alkaloids Bearing FIH Skeletons

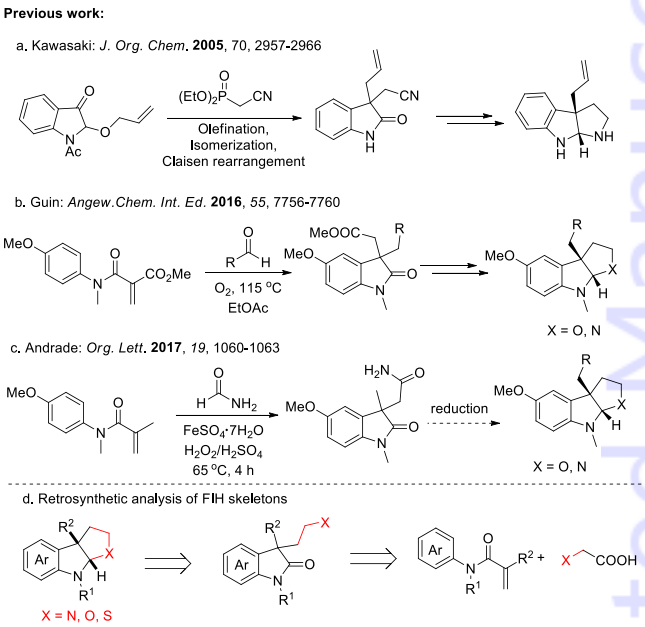

Scheme 1. Synthesis of FIH Skeletons

Due to these intriguing bioactivities, many approaches have been developed for efficient construction of the core FIH skeletons in the past decades,[1b, 5] such as 1,4-addition of Grignard reagent,[5a] Fisher indolization,[5b] domino olefination/ isomerization/Claisen rearrangement (OIC) (Scheme 1a),[5c] [4+1] cyclization,[5d] [3+2] annulation,[5f, 5g] iodine(III)-mediated intramolecular annulation,[5h] 3,3-rearrangement,[5e] Wittig olefination–Claisen rearrangement,[5i] alkyl radical (Scheme 1b) [5j] and carbamoyl radical[5k] (Scheme 1c) addition/oxidative annulation. Although all roads lead to the same destination, many drawbacks still exist such as several steps, poor overall yields, harsh conditions, pre-functionalized complex precursors or excess reagents. Particularlly, most of them can produce only one type of FIH skeleton and lack ability to construct the diversity. Hence, a unified

Table 1. Optimization of Reaction Conditions.[a]

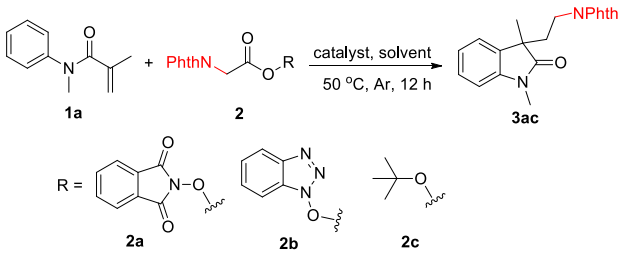

Entry	2	Cat.	Solvent	Yield (%)[b]
1	**2a**	$FeSO_4·7H_2O$	MeCN	n.r.
2	**2b**	$FeSO_4·7H_2O$	MeCN	n.r.
3	**2c**	$FeSO_4·7H_2O$	MeCN	70
4	**2c**	CuCl	MeCN	n.r.
5	**2c**	CuBr	MeCN	n.r.
6	**2c**	$FeCl_3$	MeCN	49
7	**2c**	$Fe(acac)_3$	MeCN	42
8	**2c**	Cp_2Fe	MeCN	79
9	**2c**	$FeCl_2·4H_2O$	MeCN	82
10	**2c**	$FeBr_2$	MeCN	68
11	**2c**	$FeCl_2·4H_2O$	toluene	trace
12	**2c**	$FeCl_2·4H_2O$	1,4-dioxane	trace
13	**2c**	$FeCl_2·4H_2O$	DMF	84
14	**2c**	$FeCl_2·4H_2O$	THF	n.r.
15	**2c**	–	DMF	n.r.
16[c]	**2c**	–	DMF	51
17[c]	**2c**	–	MeCN	48

[a]Reaction conditions: **1a** (0.2 mmol), **2** (0.4 mmol), cat. (0.02 mmol), solvent (1.0 mL), 50 °C, 12 h, Ar. [b]Isolated yield. [c]Performed at 100 °C.

method achieving types of FIH skeletons via a short and straightforward pattern under mild conditions is of high necessity.

Retrosynthetically, we envision that the reaction of α-heteroatom acids and *N*-methyl-*N*-arylacrylamides,[5j, 5k, 6, 7g] which are the common radical acceptors and precursors of oxindoles, via a radical addition/cyclization fashion may construct the desired oxindoles, the key intermediates to FIH skeletons (Scheme 1d).[1, 5j, 5k]

α-heteroatom acids including amino acids, glycolic acid and thioglycolic acid as the chemical feedstock, are widely employed in myriad aspects of organic chemistry. In the past decades, Ag/ persulfate system mediating decarboxylation reactions of alkyl carboxylic acids have become one of the main means to access alkyl radicals. [7] However, such system is ill-suited to α-heteroatom acids due to the ease of overoxidation of the generated radicals.[8] Recently, another protocol that uses the activated carboxylic acids to achieve alkyl radicals receives widespread attention.[9] We consider that this pre-activation strategy might serve for our design.

We initiated our investigation by screening three kind of activated glycine, reacting with *N*-methyl-*N*-arylacrylamide **1a** in the presence of $FeSO_4·7H_2O$ at

Table 2. Substrate Scope of N-arylacrylamides **1**.[a, b]

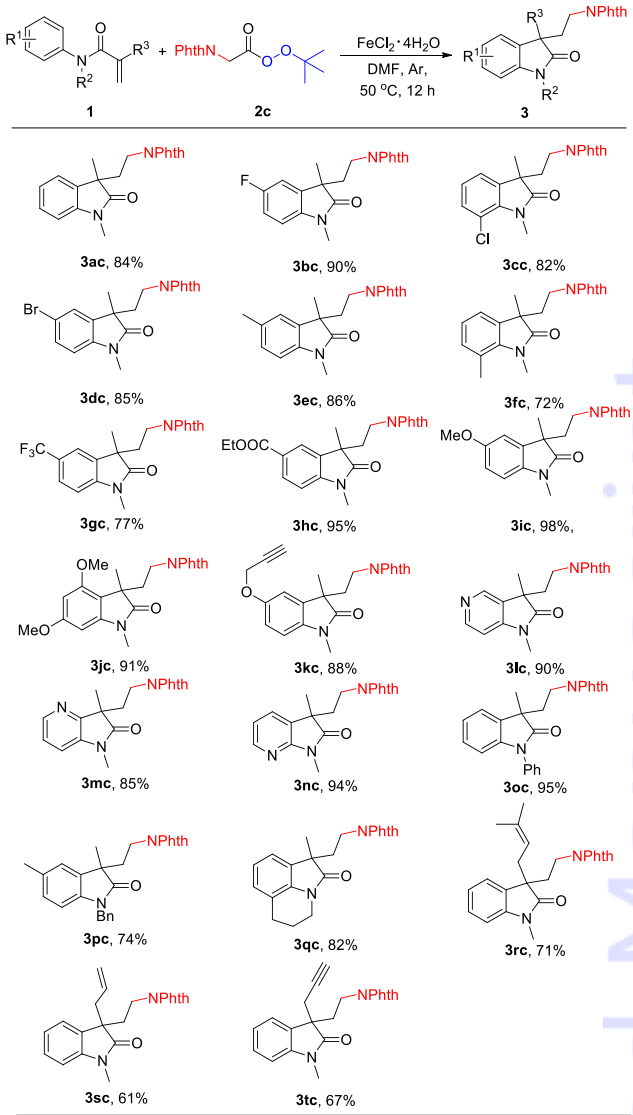

[a]Reaction conditions: *N*-arylacrylamides **1** (0.2 mmol), **2c** (0.4 mmol), $FeCl_2·4H_2O$ (0.02 mmol), DMF (1.0 mL), Ar, 50 °C, 12 h. [b] Isolated yield.

50 °C (Table 1). Smoothly as the redox-active esters **2a** and **2b** run in decarboxylative functionalizations catalyzed by iron and nickel,[9a-9d] they did not work under our reaction conditions (Table 1, entries 1 and 2). When *tert*-butyl perester **2c**[9i-9k] was employed, the expected oxindole **3ac** was obtained in 70% yield (Table 1, entry 3). Then, we chose acrylamide **1a** and *tert*-butyl perester **2c** as the model substrates to screen the metal salts and the solvents. Results of optimization of the initiators showed that Fe(II) salts outperformed Fe(III) salts (Table 1, entries 6-10) and copper salts did not initiate the reaction (Table 1, entries 4 and 5). $FeCl_2·4H_2O$ furnished the optimal outcome (Table 1, entry 9). On the other hand, the survey of solvents exhibited that DMF was superior to other solvents and gave **3ac** with a satisfactory yield (Table 1, entries 11−14). The absence of the initiator made this reaction completely shut down

Table 3. Reaction Scope of α-heteroatom acids.[a , b]

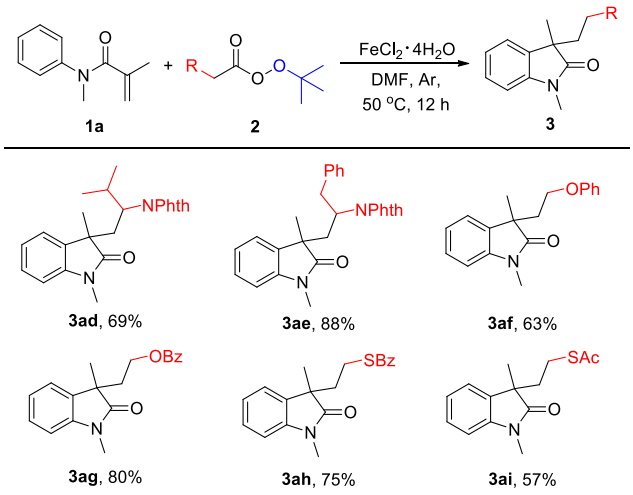

[a]Reaction conditions: *N*-arylacrylamides **1** (0.2 mmol), **2** (0.4 mmol), $FeCl_2·4H_2O$ (0.02 mmol), DMF (1.0 mL), Ar, 50 °C, 12 h. [b] Isolated yield.

(Table 1, entry 15). As the reaction was performed at the elevated temperature (100 °C) in DMF and MeCN without use of initiators, the oxindole **3ac** was achieved in moderate yields (Table 1, entries 16 and 17).

With the optimized conditions in hand, we then made an investigation of the scope of *N*-arylacrylamides **1** (Table 2). Halogens including F, Cl, Br anchoring on different position of *N*-aryl motif can be tolerated under the reaction conditions (**3bc**-**3dc**). With respect to variation of electron properties on aromatic rings, neither did the electron−withdrawing substitutes made a big difference to the reactivity (**3gc** and **3hc**), nor did the electron−donating (**3ec**, **3fc**, **3ic**-**3kc**). The existence of terminal alkyne did not alter the reaction chemoselectivity (**3kc**). *N*-pyridylacrylamides (**1l** to **1n**) were also amenable to this reaction and no alkylated pyridine products, generated through Minisci reaction pattern,[7b-7d, 7i, 9h, 10] were detected. Variation of *N*-substituents had no big effect on the reaction results (**3oc**-**3qc**). Substitutes such as allylic, prenyl or even propargyl units at the R^3 site lived in perfect harmony with the radical addition/annulation process (**3rc**-**3tc**) and no other addition byproducts were detected.

Furthermore, the substrate scope of α-heteroatom acids was also examined (Table 3). This reaction proceeded well with *tert*-butyl peresters of *L*-valine and *L*-phenylalanine, furnishing the corresponding oxindoles **3ad** and **3ae** in satisfying yields respectively (69% and 88%). *tert*-Butyl peresters of phenoxyacetic acid and glycolic acid also reacted well with *N*-methyl-*N*-arylacrylamide **1a**, affording oxindole **3af** and **3ag** in moderate yields. Notably, α-thioglycolic acid peresters smoothly underwent the radical addition/cyclization process, delivering the title products **3ah** and **3ai** in 75% and 57% yields.

All of the synthetized oxindoles above could be easily converted into FIH compounds after reduction.

Table 4. Construction of FIH Skeletons.[a , b]

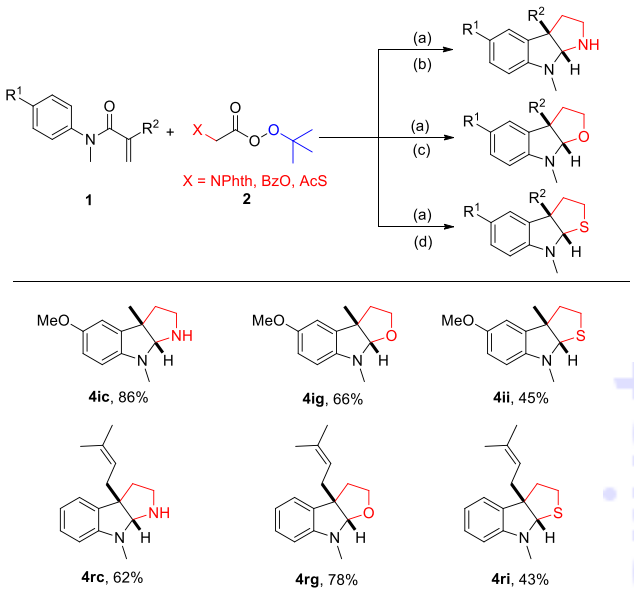

[a] Overall yield of two steps. [b]Reaction conditions: (a) $FeCl_2·4H_2O$ (0.1 equiv), DMF, 50 °C, Ar, 12 h; (b) NH_2NH_2 (10.0 equiv), MeOH; then $LiAlH_4$ (8.0 equiv), THF, 0 °C; (c) $LiAlH_4$ (8.0 equiv), THF, 0 °C; (d) $LiAlH_4$ (8.0 equiv), THF, – 60 °C.

For examples, three types of frequently-used FIH skeletons were rapidly synthesized, starting from *N*-arylacrylamides **1** and *tert*-butyl peresters of α-heteroatom acids (Table 4). A two-step sequence allowed access to hexahydropyrrolo[2,3-*b*]indole **4ic** and **4rc,** core skeletons of (±)-esermethole, (±)-physostigmine and (±)-flustramine B, (±)-flustramine E, in 86% and 62% overall yields respectively. Also, hexahydrofuro[2,3-*b*]indole skeletons **4ig** ((±)-physovenol methyl ether) and **4rg** were obtained in satisfactory yields after reduction of the generated oxindoles (**3ig** and **3rg**) by $LiAlH_4$, so were a similar two-step sequence for hexahydrothieno[2,3-*b*]indole **4ii** and **4ri.** Although thia-physostigmine exhibited stronger inhibitory activity over acetyl cholinesterase and lower toxicity than (-)-physostigmine, [2, 11] the synthetic difficulty of thienoindoline skeleton limited the further pharmacological evaluation and application. Our approach would be an ideal alternative of the previous synthetic route.[11]

To showcase the scalability, a gram−scale reaction was carried out and the corresponding oxindole **3ic** was accessed in 90% yield (Scheme 2A). It is worthy to note that evaluation of thermal stability of peresters is also of indispensability to application safety. Decomposition temperatures of the synthetic peresters measured by DSC ranged from 100 °C to 130 °C (see Supporting Information), which demonstrates that it is of relative safety to perform the gram−scale reaction under our mild conditions, but of potential danger at high temperature.

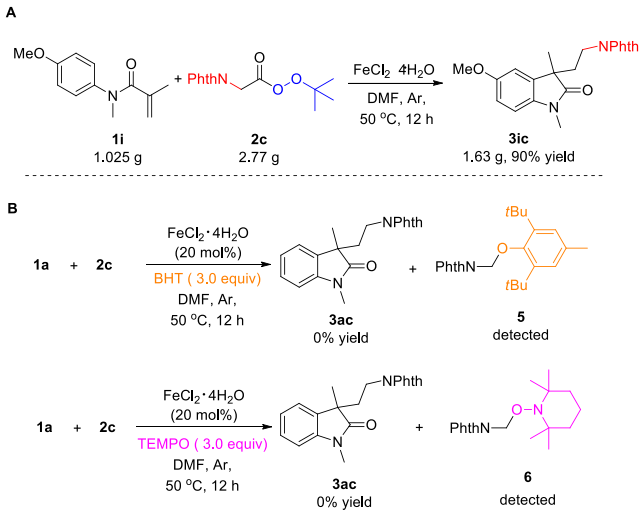

Scheme 2. (A) Gram-Scale Reaction. (B) Preliminary Investigation of Mechanism.

To probe into the plausible mechanism, radical-trapping experiments were done (Scheme 2B). Whether the reaction was conducted under the standard conditions with addition of radical scavengers BHT (3.0 equiv) or TEMPO (3.0 equiv), no oxindole **3ac** was detected by TLC and ESI-HRMS. Meanwhile, adducts **5** and **6** were successfully detected by ESI-HRMS (see Supporting Information). Based on the above experiments and literature precedence, [7k, 7l] a putative mechanism of alkyl radical addition/annulation by electron catalysis is proposed (Scheme 3).[12] The radical chain process is initiated by transferring single electron of Fe (II) to perester to deliver a reactive radical anion, which instantly generates the α-heteroatom alkyl radical **I** after cleavage of O-O bond and decarboxylation. Addition of radical **I** to *N*- arylacrylamide gives birth to the tertiary carbon-centered radical **II**. Intramolecular annulation of radical **II** with aromatic ring furnishes the radical intermediate **III,** which undergoes the single electron oxidation by perester to afford the cation intermediate **IV** and alkyl radical **I**, which further propagates the radical chain. Deprotonation of cation **IV** finally produces the oxindole.

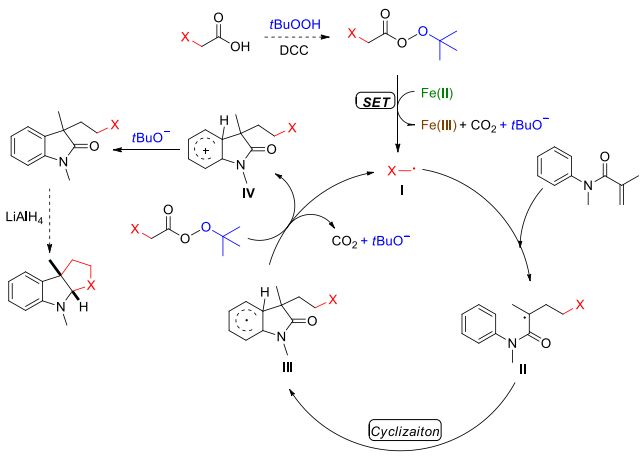

Scheme 3. Plausible Mechanism

In summary, we have developed an efficient approach to construct functionalized oxindoles via electron catalyzed radical cascade addition/annulation. This method represents a new gateway to construction of types of FIH skeletons. This method features scalability, operationally-simplicity and high degree of tolerance. From the perspective of step-economy, overall yield and synthesis diversity, our approach has strong competitive advantages over the previous methods. In fact, it is the shortest route ever reported and the first unified approach for synthesis of types of FIH skeletons.[5]

Experimental Section

General procedure for preparation of functionalized oxindoles 3

N-arylacrylamides **1** (0.2 mmol), perester **2** (0.4 mmol), and $FeCl_2{\cdot}4H_2O$ (3.96 mg, 0.02 mmol) were added into an oven-dried Schlenk tube with a stirring bar. The tube was repeatedly degassed and recharged with argon for three times. Then degassed DMF (anhydrous, 1.0 mL) was added via syringe. The resulting mixture was stirred at 50 °C for 12 h. After completion, the mixture was extracted with EtOAc for 3 times. The separated organic layer was dried over anhydrous Na_2SO_4 and concentrated under reduced pressure to furnish the crude product **3**, which was then purified by column chromatography (PE/EtOAc as eluant).

General procedure for the synthesis of pyrroloindoline skeletons

Into a 25 mL flask equipped with a magnetic stirring bar, the purified oxindole **3ic** (or **3rc)** and MeOH was placed, followed by the addition of NH_2NH_2 (10.0 equiv, 80% w/w solution in water). After stirred at room temperature for 20 h, the resulting solution was filtrated over a plug of Celite and the filter cake was washed with AcOEt for 3 times. The combined filtrate was concentrated under reduced pressure to quantitatively furnish the crude amine, which was directly placed into an oven-dried Schlenk tube without any further purification. Then, the newly-distilled THF was added through a syringe under argon. The solution was cooled to 0 °C and $LiAlH_4$ (4.0 equiv) was added portionwise over 20 min. The suspension was stirred at 0 °C for 3 h followed by another addition of $LiAlH_4$ (4.0 equiv). Then the suspension was stirred for 1h at 0 °C and 3 h at room temperature. After complete consumption of the starting material monitored by TLC, the reaction was quenched by saturated NaOH (4 drops to 10 drops) at 0 °C, followed by the addition of $MgSO_4$ and silica gel. The resulting mixture was then purified by silica gel flash column chromatography (EtOAc/MeOH as eluant) to afford the hexahydropyrrolo[2,3-*b*]indole **4ic** (or **4rc).**

Acknowledgements

We are grateful for financial support from National Natural Science Foundation of China (Grant No. 21272024).

References

[1] a) M. Somei, F. Yamada, *Nat. Prod. Rep*. **2003**, *20*, 216-242; b) For review of structure, bioactivity and synthesis of natural products bearing with pyrroloindoline skeleton, see: P. Ruiz-Sanchis, S. A. Savina, F. Albericio, M. Alvarez, *Chem. – Eur. J.* **2011**, *17*, 1388-1408.

[2] Physostigmine: K.-P. Shaw, Y. Aracava, A. Akaike, J. W. Daly, D. L. Rickett, E. X. Albuquerque, *Mol. Pharmacol*. **1985**, *28*, 527-538.

[3] a) Flustramine E and debromoflustramine B: P. B. Holsy, U. Anthoni, C. Christophersen, P. H. Nielsen, *J. Nat. Prod*. **1994**, *57*, 997–1000; b) Flustramine B: J. F. Austin, S. G. Kim, C. J. Sinz, W. J. Xiao, W. J. MacMillan, *PNAS.* **2004**, *101*, 5482-5487.

[4] For a pertinent review of physostigmine, see: D. J. Triggle, J. M. Mitchell, R. Filler, *CNS Drug Rev.* **1998**, *4*, 87-136.

[5] Selected representative examples of synthesis of FIH skeletons, see: a) M. S. Morales-Rios, N. F. Santos-Sanchez, P. Joseph-Nathan, *J. Nat. Prod.* **2002**, *65*, 136-141; b) B. W. Boal, A. W. Schammel, N. K. Garg, *Org. Lett*. **2009**, *11*, 3458-3461; c) T. Kawasaki, M. Shinada, M. Ohzono, A. Ogawa, R. Terashima, M. Sakamoto, *J. Org. Chem*. **2008**, *73*, 5959-5964; d) J. H. Rigby, S. Sidique, *Org. Lett*. **2006**, *9*, 1219-1221; e) P. F. Santos, N. Srinivasan, P. S. Almeida, A. M. Lobo, S. Prabhakar, *Tetrahedron* **2005**, *61*, 9147-9156; f) S. Lucarini, F. Bartoccini, F. Battistoni, G. Diamantini, G. Piersanti, M. Righi, G. Spadoni, *Org. Lett*. **2010**, *12*, 3844-3847; g) W. Ji, L. Yao, X. Liao, *Org. Lett*. **2016**, *18*, 628-630; h) D. Tu, L. Ma, X. Tong, X. Deng, C. Xia, *Org. Lett*. **2012**, *14*, 4830-4833; i) M. G. Kulkarni, A. P. Dhondge, A. S. Borhade, D. D. Gaikwad, S. W. Chavhan, Y. B. Shaikh, V. B. Ningdale, M. P. Desai, D. R. Birhade, M. P. Shinde, *Tetrahedron Lett*. **2009**, *50*, 2411-2413; j) P. Biswas, S. Paul, J. Guin, *Angew.Chem.* **2016**, *128*, 7887-7891; *Angew.Chem. Int. Ed*. **2016**, *55*, 7756-7760; k) V. Correia, J. Abreu, C. E. Barata, L. Andrade, *Org. Lett*. **2017**, *19*, 1060-1063; l) A. Pinto, Y. Jia, L. Neuville, J. Zhu, *Chem.–Eur. J*. **2007**, *13*, 961-967; m) B. Zhou, W. Hou, Y. Yang, H. Feng, Y. Li, *Org. Lett*. **2014**, *16*, 1322-1325.

[6] Selected representative examples of synthesis of functionalized oxindoles using *N*- arylacrylamides, see: a) J. Wang, J. Li, J. Huang, Q. Zhu, *J. Org. Chem*. **2016**, *81*, 3017-3022; b) R. Wang, W. Bao, *Tetrahedron* **2015**, *71*, 6997-7002; c) Y. Meng, L-N. Guo, H. Wang, X-H. Duan, *Chem. Commun*. **2013**, *49*, 7540-7542; d) X. Xu, Y. Tang, X. Li, G. Hong, M. Fang, X. Du, *J. Org. Chem*. **2014**, *79*, 446-451; e) B. Zhou, W. Hou, Y. Yang, H. Feng, Y. Li, *Org. Lett*. **2014**, *16*, 1322–1325; Related reviews, see: f) J.-R. Chen, X.-Y. Yu, W.-J. Xiao, *Synthesis* **2015**, *47*, 604-629; g) C.-C. Li, S.-D. Yang, *Org. Biomol. Chem*. **2016**, *14*, 4365-4377; h) J.-T. Yu, C. Pan, *Chem. Commun*. **2016**, *52*, 2220-2236.

[7] Selected representative examples of Ag/ persulfate system mediated decarboxylative functionalization, see: a) C. Ding, S. Tu, Q. Yao, F. Li, Y. Wang, W. Hu, Z. Ao, *Adv.Synth. Catal*. **2010**, *352*, 847–853; b) W.-P. Mai, B. Sun, L.-Q.You, L.-R. Yang, P. Mao, J.-W. Yuan, Y.-M. Xiao, L.-B. Qu, *Org. Biomol. Chem*. **2015**, *13*, 2750–2755; c) D. G. M. Shore, K. A. Wasik, J. P. Lyssikatos, A. A. Estrada, *Tetrahedron Lett*. **2015**, *56*, 4063–4066; d) R. Xia, M.-S. Xie, H.-Y. Niu, G.-R. Qu, H.-M. Guo, *Org. Lett*. **2013**, *16*, 444–447; e) W.-M. Zhao, X.-L. Chen, J.-W. Yuan, L.-B. Qu, L.-K. Duan, Y.-F. Zhao, *Chem. Commun*. **2014**, *50*, 2018–2020; f) J. Liu, C. Fan, H. Yin, C. Qin, G. Zhang, X. Zhang, H. Yi, A. Lei, *Chem. Commun.* **2014**, *50*, 2145–2147; g) H. Wang, L. N. Guo, X. H. Duan, *Adv. Synth. Catal*. **2013**, 355, 2222–2226; h) X. Wang, Z. Li, S. Cao, H. Rao, *Adv. Synth. Catal*. **2016**, *358*, 2059–2065. i) R. Xia, M.-S. Xie, H.-Y. Niu, G.-R. Qu, H.-M. Guo, *Org. Lett*. **2013**, *16*, 444–447.

[8] a) C. J. Cowden, *Org. Lett*. **2003**, *5*, 4497–4499; b) D N. Mai, R D. Bxter, *Org. Lett*. **2016**, *18*, 3738–3741.

[9] Selected representative examples of Fe- and Ni-catalyzed decarboxylative functionalization using Okada redox-active esters, see: a) F. Toriyama, J. Cornella, L. Wimmer, T.-G. Chen, D. D. Dixon, G. Creech, P. S. Baran, *J. Am. Chem. Soc*. **2016**, *138*, 11132-11135; b) F. Sandfort, M. J. O'Neill, J. Cornella, L. Wimmer, P. S. Baran, *Angew. Chem.* **2017**, *129*, 3367-3371; *Angew. Chem. Int. Ed*. **2016**, *56*, 3319-3323; c) T. Qin, J. Cornella, C. Li, L. R. Malins, J. T. Edwards, S. Kawamura, B. D. Maxwell, M. D. Eastgate, P. S. Baran, *Science* **2016**, *352*, 801-805; d) J. Wang, T. Qin, T.-G. Chen, L. Wimmer, J. T. Edwards, J. Cornella, B. Vokits, S. A. Shaw, P. S. Baran, *Angew. Chem.* **2016**, *128*, 9828-9831; *Angew. Chem. Int. Ed*. **2016**, *55*, 9676-9679; Selected representative examples of photoredox decarboxylative functionalization using Okada redox-active esters, see: e) K. Okada, K. Okamoto, M. Oda, *J. Am. Chem. Soc*. **1988**, *110*, 8736-8738; f) F. L. Lackner, K. W. Quasdorf, L. E. Overman, *J. Am. Chem. Soc*. **2013**, *135*, 15342-15345; g) J. Yang, J. Zhang, L. Qi, C. Hu, Y. Chen, *Chem. Commun*. **2015**, *51*, 5275-5278; h) W.-M. Cheng, R. Shang, Yao, Fu, *ACS Catal*. **2017**, *7*, 907-911; Selected examples of decarboxylation functionalization using peresters of alkyl carboxylic acids, see: i) M. R. Becerril, C. C. Sazepin, J. C. T. Leung, T. Okbinoglu, P. Kennepohl, J.-F. Paquin, G. M. Sammis, *J. Am. Chem. Soc*. **2012**, *134*, 4026-4029; j) K. R. Babu, N. Zhu, H. Bao, *Org. Lett*. **2017**, *19*, 46-49; k) W. Jian, L. Ge, Y. Jiao, B. Qian, H. Bao, *Angew. Chem.* **2017**, *129*, 3704-3708; *Angew. Chem. Int. Ed*. **2017**, *56*, 3650-3654; l) K. Foo, E. Sella, I. Thome, M. D. Eastgate, P. S. Baran, *J. Am. Chem. Soc*. **2014**, *136*, 5279-5282.

[10] Selected representative examples of Minisci reaction, see: a) F. Minisci, R. Bernardi, F. Bertini, R. Galli, M. Perchinummo, *Tetrahedron* **1971**, *27*, 3575–3580; b)

F. Minisci, R. Mondelli, G. P. Gardini, O. Porta, *Tetrahedron* **1972**, *28*, 2403–2413.

[11] The only synthetic route for synthesis of thia-physostigmine described so far, see: M. An-naka, K. Yasuda, M. Yamada, A. Kawai, N. Takamura, S. Sugasawa, Y. Matsuoka, H. Iwata, T. Fukushima, *Heterocycles.* **1994**, *39*, 251-270.

[12] Selected representative examples of electron-catalyzed reactions, see: a) D. Leifert, A. Studer, *Org. Lett*. **2015**, *17*, 386–389; b) B. Zhang, A. Studer, *Org. Biomol. Chem*. **2014**, *12*, 9895-9898; c) A. R. O. Venning, P. T. Bohan, E. J. Alexanian, *J. Am. Chem. Soc*. **2015**, *137*, 3731-3734; d) B. Janhsen, A. Studer, *J. Org. Chem*. **2017**, DOI: 10.1021/acs.joc.7b00934; e) J. Xuan, C. G. Daniliuc, A. Studer, *Org. Lett*. **2016**, *18*, 6372–6375; f) A. Biechy, S. Z. Zard, *Org. Lett*. **2009**, 11, 2800-2803; g) N. Charrier, Z. Liu, S. Z. Zard, *Org. Lett*. **2012**, 14, 2018-2021.

10.1002/adsc.201700976

COMMUNICATION

Decarboxylative Synthesis of Functionalized Oxindoles via A Iron-Initiated Radical Chain Process and Application to Construction of Diverse Fused-Indoline Heterocycls

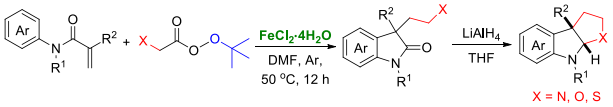

Adv. Synth. Catal. **Year**, *Volume*, Page – Page

Zhihao Cui and Da-Ming Du*